Phase Transitions and Ferroelectric Relaxor Behavior in P(VDF−TrFE−CFE) Terpolymers

Hui-Min Bao, Jiao-Fan Song, Juan Zhang, Qun-Dong Shen,* and Chang-Zheng Yang

Department of Polymer Science & Engineering and Key Laboratory of Mesoscopic Chemistry of MOE, School of Chemistry & Chemical Engineering, Nanjing University, Nanjing 210093, China

Q. M. Zhang

Materials Research Institute and Electrical Engineering Department, The Pennsylvania State University, University Park, Pennsylvania 16802

Received December 6, 2006; Revised Manuscript Received February 2, 2007

ABSTRACT: We show that the microstructures and phase transition behavior of vinylidene fluoride−trifluoroethylene−chlorofluoroethylene terpolymer, P(VDF−TrFE−CFE), with composition of 61.5/30.3/8.2 mol %, can be varied dramatically via different processing conditions. In the well-annealed sample, the polymer exhibits typical relaxor ferroelectric behavior with the nonpolar crystalline phase having a chain structure of random sequence of TT/TG/TG′ conformations. In contrast, by lowering the crystallization temperature in the solution-cast films, the polar crystal phase with all-trans ($T_{m>4}$) planar zigzag conformation (similar to the ferroelectric phase in the corresponding copolymer) can appear or even become a dominating phase. Four types of transitions can be detected in this terpolymer, besides the crystal melting, the glass transition in amorphous region, and the transition between the ferroelectric-like and paraelectric crystals (30−90 °C), an additional transition appears near 10 °C which can be attributed to the crystalline domains with all-trans sequence randomly disrupted by defects, and the coherence length of these domains is estimated to be less than 4.7 nm (polar nanodomains). The large dielectric response of the terpolymer comes from the two crystalline phases: the ferroelectric-like crystals and polar nanodomains. The former is responsible for the frequency-independent dielectric maxima while the latter generates the strong frequency dependence in the dielectric spectra, a typical feature of relaxor ferroelectrics, which we suggest to come from the short-range molecular motion in the polar nanodomains.

Introduction

Ferroelectrics are technologically important smart materials which find applications for capacitors, transducers, actuators, sensors, nonvolatile memories, and electrooptic modulators.[1−5] For over 30 years ferroelectric polymers, especially vinylidene fluoride homopolymer, PVDF, and its random copolymers with trifluoroethylene, P(VDF−TrFE)s, have drawn considerable attention.[6−14]

P(VDF−TrFE)s are semicrystalline fluorinated polymers which although having simple chemical structures, $-(CH_2-CF_2)_x-(CHF-CF_2)_{1-x}-$, exhibit rather complicated crystalline structures and morphologies.[6,15] Their interesting electric properties originate from the molecular conformation and the chain packing in the crystalline regions. P(VDF−TrFE) crystals with all-trans ($T_{m>4}$) planar zigzag conformation and parallel electric dipole moments are ferroelectrics and exhibit a spontaneous electric polarization that can be switched from one direction to another by the external electric field. The P(VDF−TrFE) crystals formed by a statistical combination of TG, TG′, TTTG, and TTTG′ molecular conformations are paraelectric, which has total dipole moment in the crystal zero. The structural transition from ferroelectric to paraelectric crystals leads to significant changes of dielectric constant, piezoelectric and pyroelectric coefficients, and the lattice constant of the P(VDF−TrFE)s.

Recently, it was discovered that properly electron-irradiated P(VDF−TrFE) displays an electric field-induced longitudinal strain of about 4%, which makes it valuable for high-performance electromechanical devices.[13] Further investigation provides an alternative way to obtain fluorinated polymers with large electromechanical response. The random incorporation of a small amount of ternary monomers with bulky groups, such as chlorotrifluoroethylene (CTFE), 1,1-chlorofluoroethylene (CFE), and hexafluoropropene (HFP), into main chains of P(VDF−TrFE)s affords the fluorinated ternary polymers with field-induced strain to more than 7%.[16−20] Besides the electromechanical response, there is remarkable difference in the thermal and electric behaviors between the P(VDF−TrFE)s and the terpolymers. The most distinctive feature is that some terpolymers show strong dielectric peak (dielectric constant >50) near room temperature and the peak shift progressively to higher temperature. This is different from the copolymer, a normal ferroelectric material, in which the ferroelectric−paraelectric transition does not show much frequency dependence.

The strong frequency dispersion of the fluorinated terpolymers is considered as a universal feature of the relaxor ferroelectrics, which are mostly found in inorganic compounds with complex composition and have attracted a great deal of attention in recent years.[21−24] Classical relaxor ferroelectrics, such as lead magnesium niobate and lanthanum-doped lead zirconate titanate ceramics, are characterized by broad frequency dispersion in the complex dielectric constant, slowing dynamics, and logarithmic polarization decay.[25] Their unusual relaxor behaviors are considered as a result of heterogeneous nanoscale polar crystalline regions where the energy barriers to reorientation are comparable to the energy of thermal motion. However, the diffuse phase transition in the semicrystalline fluorinated terpolymer has not been fully understood, since both the crystalline and amorphous regions can attribute to the dielectric

* Corresponding author: Ph 86-25-83317807; Fax 86-25-83317761; e-mail qdshen@nju.edu.cn.

10.1021/ma062800l CCC: $37.00
Published on Web 03/03/2007

relaxation process. The situation is further complicated by the factors that electric properties of the terpolymers are dependent on the crystallization conditions and other processing conditions.[26−29]

In this paper, we investigate the phase transition and relaxation behavior of the P(VDF−TrFE−CFE) terpolymer with high CFE content (8.2 mol %). Early studies have indicated that, at this condition, the ferroelectric phases are nearly eliminated, and the ferroelectric-to-paraelectric transition can hardly be detected.[27] In this study, it will be shown that under certain processing conditions a metastable ferroelectric-like phase can coexist with nonpolar phase or even become the predominant phase in the crystalline region of the P(VDF−TrFE−CFE) sample. The results indicate a complex energy surface in the terpolymers with very small energy difference between different molecular conformations, which combined with crystallization kinetics leads to the formation of many metastable phases. Hence, by varying the processing condition, the content of different phases can be varied in the same polymer which provides an opportunity to study polymeric relaxor ferroelectrics, especially in the detailed microstructures, and their influence on electric and mechanical properties. Experimental data to be presented suggest that the ferroelectric relaxor behavior originates from the short-range molecular motion in the polar nanodomains.

Experimental Section

P(VDF−TrFE−CFE) (61.5/30.3/8.2 mol %) was synthesized by a suspension method.[30] For the comparison, P(VDF−TrFE) (68/32 mol %) purchased from Solvay and Cie, Bruxelles, Belgium, was also studied.

Preparation of the Films for Measurement. To vary the microstructure of fluorinated terpolymer, the samples are treated at different crystallization conditions as follows. (1) Crystal growth from solution at low temperature: a predetermined amount of the fluorinated polymer was fully dissolved in *N*,*N*-dimethylformamide (DMF) to make a homogeneous solution with a concentration of 50 mg/mL. The solution was poured onto a glass slide and dried in air at 30 °C for 24−48 h. The obtained film was then dried under vacuum at 30 °C for at least 3−4 days (the films are referred to as terpolymer SG30). (2) Crystal growth from solution at moderate temperature: the film was prepared by the same procedure as the method 1, except that the solvent evaporation and crystallization temperature is 60 °C (the films are referred to as terpolymer SG60). (3) Crystal growth at high temperature: the as-prepared film by method 2 was annealed at 110 °C in a vacuum for 24 h and then slowly cooled down to room temperature (the films are referred to as terpolymer annealed).

Characterization. The wide-angle X-ray diffraction measurement was performed using an X'Pert Pr X-ray diffractometer (Philips) with a wavelength of 1.5418 Å. The heating rate is 2 °C/min for the XRD measurement. The FT-IR experiment was carried out using a Bruker IFS-66V Fourier transform IR spectrophotometer at 2 cm^{-1} resolution with 200 scans. Differential scanning calorimetry (DSC) was conducted on a Perkin-Elmer Pyris 1 DSC calorimeter with a heating rate of 20 °C/min. The dielectric spectroscopy was acquired using an HP4194A impedance analyzer, with a heating rate of 2 °C/min and frequency from 100 Hz to 1 MHz. Circular gold electrodes (about 40 nm thick and 1.4 mm radius) were sputtered in the center area on both surfaces of each sample. The dynamic mechanical thermal analysis (DMTA) data were collected with DMTA V (Rheometric Scientific, Inc.) at 1 and 10 Hz at a heating rate of 3 °C/min.

Results and Discussion

Ferroelectric-like Phase in the Terpolymer. Figure 1 presents the XRD data for the terpolymers at near the {110, 200} reflection. The terpolymer annealed sample exhibits one narrow peak at 18.00° with the interchain crystal space (*d*) of 4.93 Å. This lattice parameter of the terpolymer is similar to that of the {110, 200} (4.88 Å) reflection in the paraelectric crystal of P(VDF−TrFE) (52/48 mol %) which has a disordered 3/1 helical structure and TG/TG′ conformation.[15] For comparison, we also present the XRD pattern for the P(VDF−TrFE) 68/32 film prepared by similar processing conditions, i.e., growth from DMF solution at 60 °C followed by thermal annealing of as-prepared sample at 140 °C which has a {110, 200} reflection at 19.88° with lattice parameter of 4.47 Å, as expected for the ferroelectric crystalline phase where the chain conformation is all-trans ($T_{m>4}$) planar zigzag.

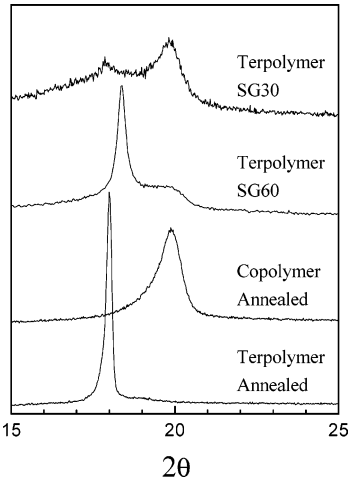

Figure 1. Room temperature X-ray diffraction pattern of the copolymer [P(VDF−TrFE) 68/32] and the terpolymer [P(VDF−TrFE−CFE) 61.5/30.3/8.2] with different processing conditions.

Although thermal annealing is one of the effective processes to enhance the crystallinity and ferroelectric properties of fluorinated copolymer, it is adverse to the formation of ferroelectric crystals in P(VDF−TrFE−CFE) 61.5/30.3/8.2. In contrast, the crystalline regions in the thermally annealed terpolymer are nonpolar. Obviously, the incorporation of chlorofluoroethylene units into P(VDF−TrFE) plays an important role in destabilization of the ferroelectric phases in the terpolymer.

Su and Strachan suggested that, in perfect P(VDF−TrFE) crystals, all-trans planar zigzag conformations are preferable than the others as a result of better interchain packing and larger cohesive energy, while the TGTG′ conformation is more stable in the isolated copolymer chain.[31] Since the van der Waals radius of chlorine in CFE is larger than fluorine, the chains in the P(VDF−TrFE−CFE) crystals have to adjust their spacing to accommodate the bulky ternary monomers. It is found that lattice parameter of {110, 200} reflection in the paraelectric crystals of the terpolymer is larger (0.05 Å) than that of the copolymer. Another side effect of CFE is that their random distribution along the chains disrupts the interchain interaction. More structure defects in the terpolymer crystals are expected. The crystallinity is estimated to be 74.8% and 54.0% for the thermally annealed P(VDF−TrFE) and P(VDF−TrFE−CFE), respectively. The expansion of the interchain lattice spacing and weakened interchain interaction are favorable to the introduction of gauche state into the isolated terpolymer chains. Therefore, the relative energetic stability of the ferroelectric and paraelectric phases in the terpolymer is relevant to the content of CFE.

On the basis of the thermodynamic approach known as Landau−Ginzburg−Devonshire theory, the free energy curves

Scheme 1. Relationships between Free Energy and Electric Polarization of the Polymers

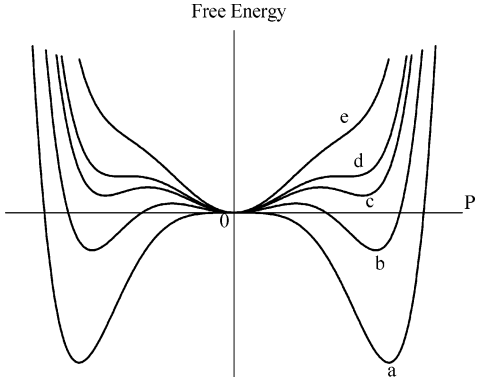

for the above-discussed polymers at ambient temperature in the absence of external electric field are described in Scheme 1. The most stable phases are ferroelectric in the thermally annealed P(VDF−TrFE) with energy minima at the polarization (P) of $\pm Ps$ (curve a). The paraelectric crystals ($P = 0$) in the copolymer are much higher in energy and thermodynamically unstable phase. Adding CFE into the copolymer gradually destabilizes the ferroelectric phases (curve b). The relative energetic stability of the ferroelectric and paraelectric phases is reversed at higher CFE content (curves c, d). Finally, the ferroelectric phases are eliminated (curve e). X-ray data indicate the thermally annealed P(VDF−TrFE−CFE) with 8.2 mol % CFE has free energy minimum at zero polarization (paraelectric phase). However, it is possible that ferroelectric phase can coexist as metastable phases with paraelectric one under certain conditions, as shown in curves c and d.

For the terpolymer solution-grown at 60 °C without further thermal annealing process, labeled as terpolymer SG60, the diffraction peak at 18.4° (4.82 Å) indicates {110, 200} reflections of the paraelectric phase (Figure 1). It is noteworthy that there is a broad shoulder located at ca. 19−20°. The best fitting to the curve reveals the shoulder is the superposition of two independent peaks, one at 19.2° (4.62 Å) and the other near 19.9° (4.46 Å). The P(VDF−TrFE) copolymer is also reported to show an overlap of two peaks with different crystallographic modification, i.e., molecular conformation and the chain packing. They have been identified as ferroelectric crystalline forms named as "low-temperature" (LT) phase with parallel arrangement of CF_2 dipoles of planar zigzag chains and "cooled" (CL) phase with more disordered packing of long trans chains interrupted by some gauche segments.[6,32] Accordingly, the doublet in terpolymer SG60 is assigned to a less-ordered planar-zigzag structure and a well-ordered all-trans state. These phases may be regarded as polar phases or ferroelectric-like phases to distinguish them from the macroscopic ferroelectric phase in the copolymers. This is direct evidence of the presence of the ferroelectric crystals as the metastable phase (Scheme 1c) in crystalline regions of P(VDF−TrFE−CFE) terpolymers with high CFE content. The result suggests that the ferroelectric terpolymer crystals prefer to grow from the solution at low temperature rather than in the bulk state as annealed at high temperature. In fact, as the temperature is further lowered to below room temperature, the ferroelectric phase will be preferred compared with the nonpolar phase. Under high electric fields, the macroscopic ferroelectric phase can be formed in the relaxor polymers as has been observed in an earlier experiment.[13]

Consistent with these observations, in the terpolymer solution-grown at 30 °C (labeled as terpolymer SG30) the ferroelectric-like phase becomes predominant over the paraelectric one as indicated by the XRD data, where a broad {110, 200} reflection is observed at the peak position for the ferroelectric phase (∼19.8°), while the {110, 200} reflection appears as a broad shoulder at 18.0°, corresponding to a nonpolar phase.

Table 1. Lattice Constant and Coherence Length for the {110, 200} Reflection of the Terpolymer Treated with Different Methods

	crystallinity, %	ferroelectric phase		paraelectric phase	
		d, Å	L, nm	d, Å	L, nm
terpolymer annealed	54.0			4.93	37.6
terpolymer SG60	35.4	4.62	5.8	4.82	25.9
		4.46	11.1		
terpolymer SG30	31.0	4.46	9.1	4.91	2.8

The above discussion indicates that the crystal structure of terpolymer is determined by two factors: thermodynamics and kinetics. The nonpolar phase in terpolymer 61.5/30.3/8.2 is the thermodynamic stable phase, but some kinetic factors can induce the polar phase or ferroelectric-like phase. One consideration is that nucleation at low temperature will lead to slow crystal growth rate. This may favor the formation of orderly packed ferroelectric crystals rather than the disordered ones with a chain structure of random sequence of TT, TG, and TG′. The solvent may also change the relative stability among different conformations. It was reported that the formation of ferroelectric phase in PVDF homopolymer is controlled by the nature and composition of the solvents.[33,34] Dipole interactions between polar solvent expand the random chain coils to obtain polymer conformations including more trans states. On the other hand, the polar small molecules are helpful to stabilize the as-grown polar ferroelectric crystals by lowering the energy of the charged surface. For nonpolar paraelectric crystal, such an effect is unavailable. When acetone (dipole moment 2.88 D) is chosen instead of DMF (3.82 D), the terpolymer crystals solution-grown at 30 °C afford the same structure; i.e., the ferroelectric-like phases are dominant. Elevation of the temperature of solution crystallization reduces the polarity of solvents and results in a more coiled chain. More gauche states are introduced into a long trans sequence. Therefore, the crystals change from well-ordered ferroelectrics (LT phase) to less-ordered ones (CL phase). This qualitatively explains the difference between the crystal structure of terpolymer SG60 and SG30. It can be postulated that, above certain temperature, the polar ferroelectric crystals will be finally replaced by the nonpolar ones, like that in the thermally annealed terpolymer.

The structural data of the terpolymer handled at different conditions are summarized in Table 1. The crystallite sizes or coherence lengths (L) perpendicular to {110, 200} crystallographic plane, corresponding to the sizes of polar or nonpolar domains, are estimated using the Scherrer equation:

$$L = \frac{0.9\lambda}{B\cos\theta} \tag{1}$$

where λ is X-ray wavelength and B and θ are full width at half-maximum (in 2θ) and angular position of the diffraction peaks, respectively. The coherence lengths of paraelectric phases significantly decrease from 37.6 to 2.8 nm with lowering crystallization temperature (Table 1) and are coincident with the order of the crystallinity. In contrast, the dimensions of well-ordered ferroelectric phases in the terpolymers are almost the same. The coherence length in terpolymer SG30 is 9.1 nm, very close to that in terpolymer SG60, while the less-ordered ferroelectric phases in terpolymer SG60 are appreciably smaller than the well-ordered ones.

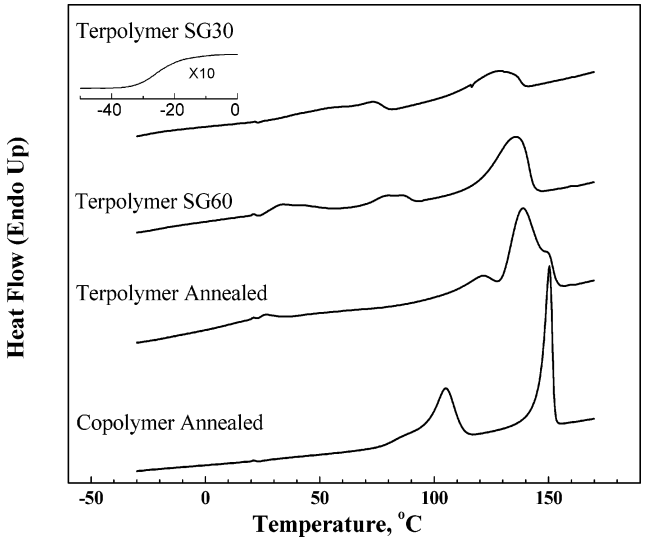

Figure 2. DSC curves for the copolymer and terpolymers.

Hence, the crystalline structures of the terpolymer SG30 (or SG60) are different from the thermally annealed terpolymer. The coexistence of ferroelectric and paraelectric phases in terpolymer SG30 is the characteristics of the normal ferroelectrics with sharp first-order ferroelectric−paraelectric phase transition; i.e., there is a discrete jump of spontaneous polarization at phase transition temperature accompanied by the changes of chain conformation and crystalline structure, while the annealed terpolymer is generally regarded as relaxor ferroelectrics with diffuse phase transition and distinctive properties from normal ferroelectrics. The structure origin of relaxor behavior is ambiguous until now. Following free energy curve a to curve d in Scheme 1, one may expect that large ferroelectric crystals are gradually broken into smaller ones and finally replaced by the paraelectric crystals. Among the last stage, it is possible that the crystals have degree of order between ferroelectrics and paraelectrics. In view of this, monitoring the interspecies transition between the terpolymer with different structure will disclose more facts behind the relaxor ferroelectrics.

Ferroelectric−Paraelectric Phase Transition in the Terpolymers. Thermal analysis results are shown in Figure 2. The endothermal melting peaks of terpolymer thermally annealed, SG60, and SG30 are found at 139, 135, and 129 °C, respectively. The melting temperatures of the terpolymers are directly relevant to the crystallinity and the paraelectric crystallite sizes. In thermally annealed P(VDF−TrFE) with a composition of 68/32 mol %, the structure transition from a ferroelectric crystal to paraelectric one results in the appearance on the DSC curve of an endothermal peak with its maximum at 105 °C (Figure 2). Contrarily, the endothermal peak at 26 °C, corresponding to ferroelectric−paraelectric phase transition of thermally annealed P(VDF−TrFE−CFE), is hardly discernible. The evidence supports the previous observation that paraelectric phases are predominant in crystalline region of the annealed terpolymer, and only a trace amount of ferroelectric phase is detectable.

In the temperature interval being studied, two phase transitions (25−60 and 65−90 °C) in terpolymer SG60 are observed in addition to the melting peak (Figure 2). The multiplicity of endothermal peaks can be the consequence of the following: (1) Structural factor: Two ferroelectric phases with different molecular conformation and the chain packing. For example, P(VDF−TrFE)s can have polymorphic transitions from CL and LT phases to paraelectric phase, respectively. (2) Size effect: The ferroelectric phases of two or more sizes. (3) Defect content: Two crystalline regions with different chemical compositions, where one with lower CFE fraction is in favor of the formation of well-ordered ferroelectric phase and the other with more inclusion of termonomer makes for less-ordered ferroelectric phase.

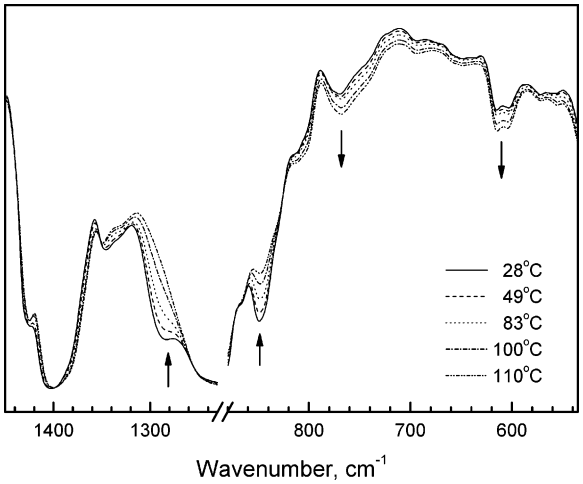

Figure 3. Temperature dependencies of the IR spectra for terpolymer SG60 during the heating process.

To clarify the structure origination of multiple phase transition at temperatures well below melting point, one must also resort to X-ray and other techniques. As has been discussed, phase transitions in the P(VDF−TrFE−CFE) crystal should also be reflected by the molecular conformational change. Detailed interpretation of the vibrational spectra of PVDF and its copolymers with various crystalline modifications enables the reasonable assignment of the absorption bands to the characteristic sequences of trans and gauche states.[32,35−37] FTIR spectra of terpolymer SG60 are investigated in a temperature range of the multiple crystal−crystal transitions revealed by thermoanalysis. As shown in Figure 3, there are obvious temperature dependencies of the infrared absorption intensities in terpolymer SG60. Crystal bands at 1283 and 848 cm^{-1} corresponding to all-trans ($T_{m>4}$) conformation decrease remarkably in intensity with the elevation of temperature, while the absorbance at 768 and 614 cm^{-1} for TG conformation increases in turn.

Infrared absorption intensities as a function of sample temperatures during heating process are displayed in Figure 4c. These data provide valuable information regarding two phase transitions seen by calorimetry at 25−60 and 60−90 °C (Figure 4a). For the first transition, there is a steady decrease in all-trans states along with continually enrichment in TG sequences. In contrast, although the all-trans components are further reduced during the secondary transition, the contents of TG sequences are hardly affected by the temperature.

Influence of the heating on X-ray diffraction pattern of terpolymer SG60 is monitored (Figure 5). The {200, 110} reflections of the paraelectric phase continuously increase in height and move toward lower angles as a result of thermal expansion. The intensities of diffraction peaks from ferroelectric phases drop quickly during heating process and disappear at temperature higher than 80 °C. Separation of two independent ferroelectric peaks at ca. 19.2° and 19.9° by curve fitting gives more insight into the structure change. As shown in Figure 4b, the temperature dependence of the paraelectric phase, well-ordered ferroelectric phases, and less-ordered ferroelectric phases can be divided into two regions, which fall into exactly the same temperature ranges given by DSC and FTIR analysis. In the first region, there is a significant reduction in diffraction intensity

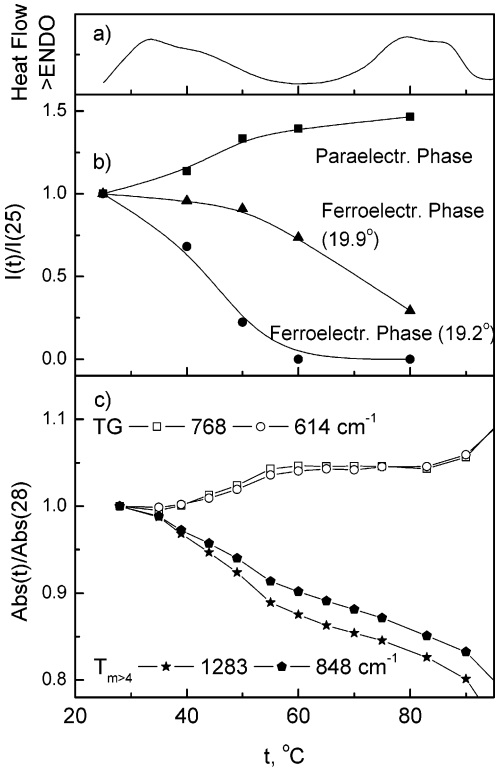

Figure 4. Changes of (a) heat flux, (b) X-ray reflection intensity, and (c) infrared absorption in terpolymer SG60 during the heating process. The latter two use the scan taken at 25 and 28 °C as reference, respectively.

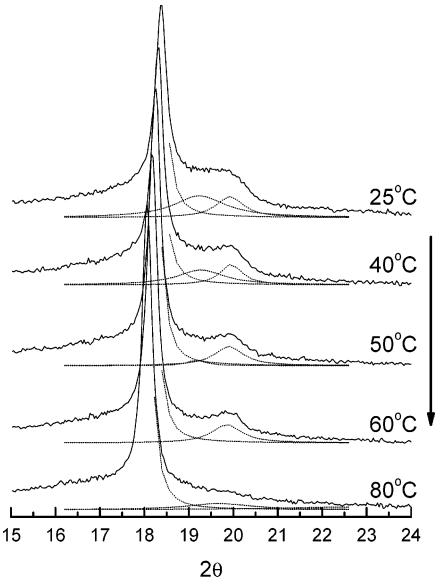

Figure 5. Temperature dependencies of the X-ray diffractograms for terpolymer SG60 during heating process. Dotted lines are the curve-fitting results.

of the less-ordered ferroelectric phases paralleled with the increase in peak corresponding to the paraelectric phase. The well-ordered ferroelectric phases are unaltered. Therefore, the transition from less-ordered ferroelectric phases to paraelectric phase should account for most of endothermal process between 25 and 60 °C. In the second region, the rise of paraelectric peaks is achieved at the cost of intensity reduction of well-ordered ferroelectric phases. In other words, the thermal change over the temperature ranging from 60 to 90 °C should be ascribed to continuous transition between the well-ordered ferroelectric phases and the paraelectric ones.

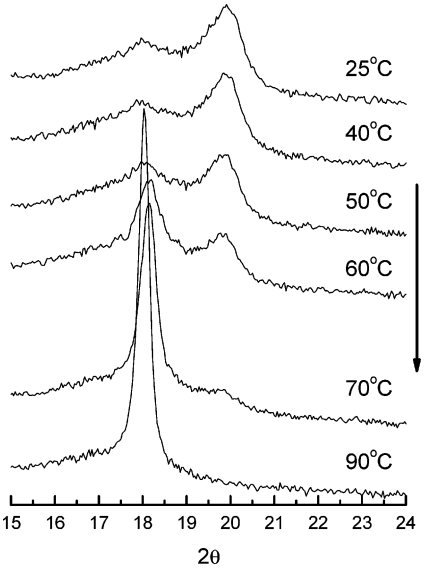

Figure 6. Temperature dependencies of the X-ray diffractograms for terpolymer SG30 during the heating process.

Double ferroelectric−paraelectric transitions in terpolymer SG60 should also be relevant to the bimodal distribution of ferroelectric crystalline regions with coherent domain sizes of about 6 and 11 nm, respectively. It was reported that a significant change of P(VDF−TrFE) ferroelectric domain sizes occurs during annealing at temperature (T_A) around T_c. Larger domains ($T_c > T_A$) grown further at the expense of the shrinkage of the surrounding smaller domains ($T_c < T_A$). The annealing process leads to the well separation of enlarged and contracted domains.[38] This may explain why terpolymer SG60 has ferroelectric crystals with T_c higher and lower than growth temperature. The size effect in the ferroelectric−paraelectric phase transition temperature or Curie temperature (T_c) has been studied and expressed as

$$T_c = T_c(\infty)\left(1 - \frac{\sigma}{AL}\right) \tag{2}$$

where σ is the surface free energy, L is the coherence length of ferroelectric phase, A is a constant, and $T_c(\infty)$ is the Curie temperature of infinite size ferroelectrics.[39] Using eq 2 and the experimental data for the two transitions in terpolymer SG60, $T_c(\infty)$ is estimated at 403 K (130 °C).

It is also possible that the two ferroelectric crystalline regions in terpolymer SG60 have different chemical compositions. The lattice constants of well-ordered ferroelectric phases in terpolymer SG60 and P(VDF-TrFE) 68/32 are pretty close (4.45 and 4.46 Å), suggesting few inclusion of the CFE in these crystalline regions. It would be likely that the less-ordered ferroelectric phases have relatively high CFE content.

In marked contrast to terpolymer SG60, terpolymer SG30 presents a broad ferroelectric−paraelectric phase transition between 30 and 70 °C (Figure 2). Temperature dependence of the XRD diffraction peaks shows that the crystal structures are unchanged below 40 °C. The remarkable intensity reduction of the reflections connected with ferroelectric crystals is observed above 50 °C (Figure 6). It is accompanied by an extraordinarily fast rise at diffractions from paraelectric crystals. When temperature rises from room temperature to 90 °C, the paraelectric phases show at least 10-fold increase in size ($L_{\{110,\ 200\}}$), from 2.8 to 28.6 nm. In comparison, the paraelectric crystal in terpolymer SG60 only grows from 25.9 nm (25 °C) to 30.2 nm (80 °C). The observation strongly suggests that ferroelectric

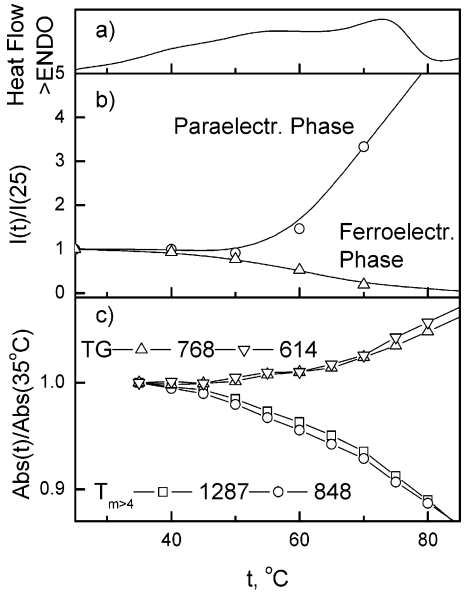

Figure 7. Temperature dependence of (a) heat flux, (b) X-ray reflection intensity, and (c) infrared absorption in terpolymer SG30 during the heating process. Reference temperatures are 25 and 35 °C for XRD and FTIR measurements, respectively.

regions in terpolymer SG30, with an average size of about 9−10 nm, merge into larger paraelectric domains during the phase transition. The gradual conversion between the ferroelectric and paraelectric crystals supports that terpolymer SG30 undergoes a first-order phase transition.

FTIR analysis reveals that the ferroelectric−paraelectric phase transition of terpolymer SG30 takes place at temperature above 40 °C with an increase in the number of high-energy TG conformations and a decrease of extended all-tans ($T_{m>4}$) conformation in the crystal (Figure 7). The tendency is coincident with that observed by XRD. Dissimilar to the case of terpolymer SG60, it is hard to separate two independent structure transition in terpolymer SG30 by spectroscopic methods, though the thermal analysis implies the existence of a small shoulder at 56 °C besides the endothermic peak at 73 °C. Nevertheless, the consolidation of two contiguous transitions is still a possible option. Using eq 2, T_c for terpolymer SG30 is calculated to be 68.5 °C, close to what is observed by DSC.

Irreversibility of the Ferroelectric Phase Transition. Figure 8 displays X-ray diffraction pattern taken during cooling process of terpolymer SG30. The peak of paraelectric phase gradually moves to high degree due to the shrinkage of the lattice. The sample does not give any characteristic reflections from ferroelectric crystalline form until cooling down to room temperature, where it exhibits an appreciably ferroelectric peak around 19.5°. DSC traces of the heating and cooling cycle are also shown (inset of Figure 8). On cooling of terpolymer SG30, one exothermal peak at 31 °C is observed, corresponding to the subsequent formation of extremely small amount of ferroelectric phase. The nucleation of ferroelectric crystals from paraelectric matrix results in the formation of numerous interphase boundaries. The fast motion of the boundaries and the evolution of heat near paraelectric−ferroelectric phase transition temperature lead to the less-ordered stacking of lamellar crystals, more rotatory isomers (gauche state) on the surface of the crystallites and along the polymer chains, and the twist of the phase boundaries. In such a circumstance, the less-ordered ferroelectrics are energetically more favorable than the well-ordered ones. The reheating of terpolymer SG30 monitored by DSC is found to differ from the first heating process with a considerably lower

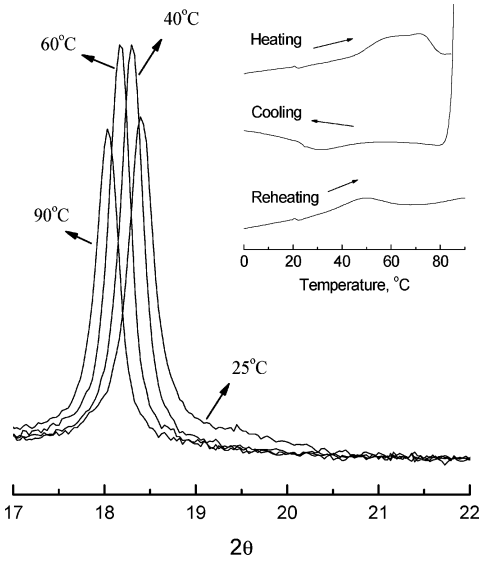

Figure 8. Temperature dependencies of the X-ray diffractograms for terpolymer SG30 during cooling process. Inset: DSC traces of the heating and cooling cycle.

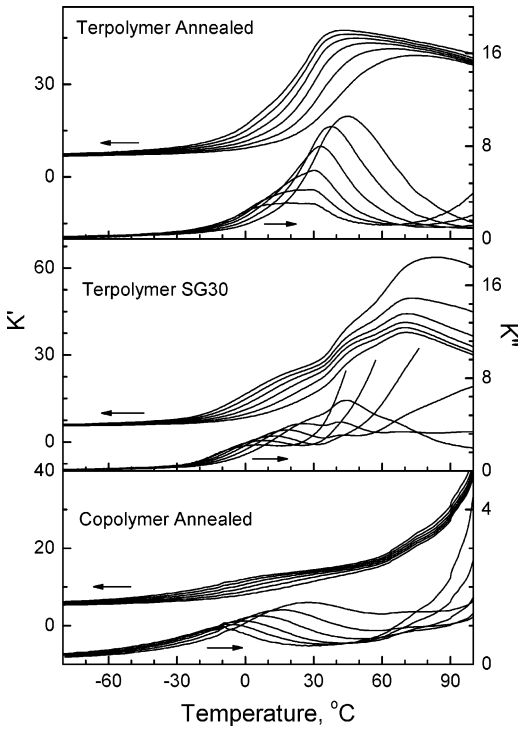

Figure 9. Dielectric spectra of the polymers at different frequencies. Curves from left to right: 10^3 to $10^{5.5}$ Hz at intervals of $10^{0.5}$ Hz.

Curie temperature (50 °C), which supports that the frozen ferroelectric crystals are less-ordered in molecular structure.

Relaxation Behaviors in the Terpolymers. As shown in Figure 9, the real and imaginary parts of dielectric constant (K' and K'') of thermally annealed terpolymer shows a rather broad peak which shifts progressively with frequency toward higher temperature. On the other hand, in the case of terpolymer SG30, the dielectric spectra changes in a different manner. At least two transitions are discernible. The first one at temperature below 40 °C is strongly frequency dependent, while the dielectric maximum of the second transition is nearly frequency independent, which suggests a ferroelectric−paraelectric transition as that observed in the normal ferroelectric copolymer, except here the transition is much broader. This is consistent with the XRD data as shown in Figure 6.

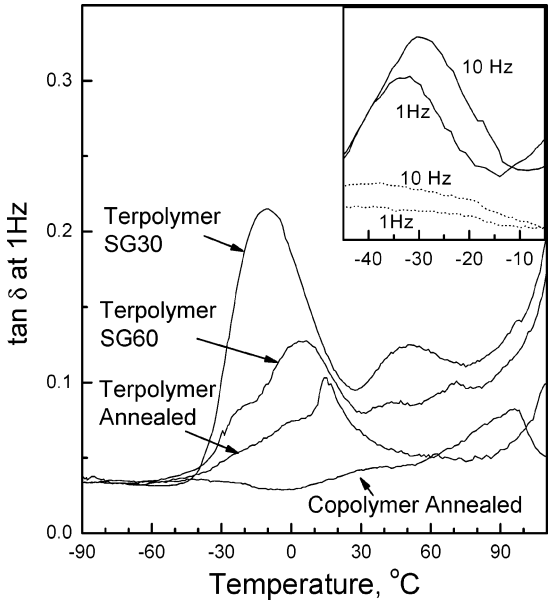

Figure 10. DMTA curve of the polymers measured at 1 Hz. Inset: mechanical loss tangent of the copolymer solution growth at 60 °C (solid line) and thermally annealed (dotted line).

The frequency dependence of permittivity, or so-called dielectric relaxation, in terpolymer thermally annealed is a topic of some delicacy. It is generally considered as distinct characteristics of relaxor ferroelectric, an exceptional type of crystals or ceramics in which dielectric constant can be as high as 10^{4-5}. A dielectric constant above 40 at 100 Hz and ambient temperature is observed in the thermally annealed terpolymer, while conventional polymers have dielectric constant less than 10. There is an open question on whether the ferroelectric relaxor state is a ferroelectric state broken up into domains of nanosize or a dipolar glass state with randomly interacting polar microregions.[22,23] An alternative consideration is that the relaxation originates from amorphous regions rather than crystalline region.[28] It correlates with segmental motion and gives rise to glass transition in semicrystalline polymers.

The mechanical loss (tan δ) vs temperature curves are shown in Figure 10. The glass transition temperature (T_g) of PVDF is reported to −40 °C and incorporating TrFE into PVDF slightly shifts it to high temperature.[11] Dynamic mechanical thermal analysis reveals that P(VDF−TrFE) 68/32 as-cast from DMF solution exhibits a relaxation transition at −33 °C (1 Hz), which is greatly suppressed in intensity and shift to −41 °C (1 Hz) after thermal annealing (inset of Figure 10). The relaxation can be interpreted by a common mechanism that the micro-Brownian motion of polymer main chain takes place in amorphous regions.

For P(VDF−TrFE−CFE), several mechanical loss peaks were observed with increasing temperature. For convenience of discussion, these peaks are divided into two groups. In the temperature region between 30 and 90 °C, there are peaks in terpolymers SG30 and SG60 corresponding to the ferroelectric−paraelectric phase transition. Another set of peaks are the lower temperature ones, which in the terpolymer SG60 is the superposition of two anomalies, locating at −23 and 3 °C (1 Hz). The broad and frequency-dependent peak in terpolymer SG30 also consists of two overlapping peaks at −19 and −3 °C (1 Hz). For the thermally annealed terpolymer, these transitions are observed at −19 and 10 °C at 1 Hz. The DSC measurement during heating process of terpolymer SG30 and SG60 shows an inflection at −26 and −24 °C, respectively, which indicates glass transition at these temperatures. Thereby,

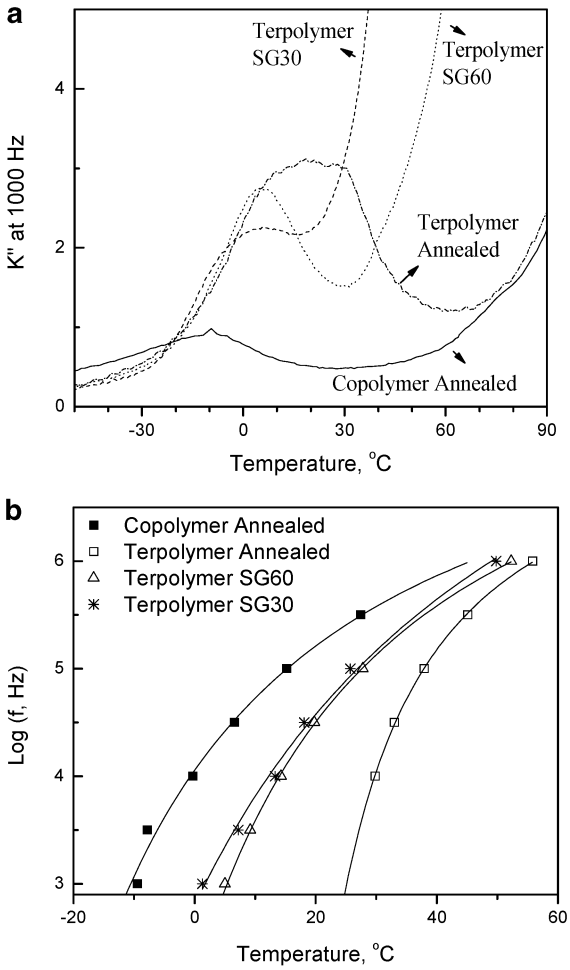

Figure 11. (a) Dielectric loss curve for various polymer and (b) frequency dependence of transition temperature in the polymers. Also indicated is the curve fitting by the Vogel−Fulcher equation.

the transitions in glass state of the terpolymers are assigned to the relaxations below −20 °C, rather than that around 0 °C.

As shown in Figure 9, thermally annealed P(VDF−TrFE) exhibits dielectric relaxation of main chain in amorphous state. For the thermally annealed terpolymer, the dielectric loss peak is also frequency dependent. It seems that the frequency-dependent dielectric response in the terpolymer is a result of segmental motion in the amorphous phase. However, careful examination provides evidence adverse to this hypothesis. First, among three terpolymer samples, terpolymer SG30 has the highest content of amorphous state (69%) but lowest dielectric loss (Figure 11a). This implies that increasing the crystallinity of the terpolymers gradually enhances the dielectric loss peaks. Second, dielectric relaxation of thermally annealed terpolymer appears at temperature higher than that of terpolymer SG30 and SG60 and far from T_g of copolymer (Figure 11b), which suggests that the diffuse phase transition temperature increases with the crystallinity in the terpolymer.

As shown in Figure 11b, the shift of dielectric peak temperatures with frequency follows the empirical Vogel−Fulcher equation:

$$\ln\left(\frac{f}{f_0}\right) = -\frac{U}{k_B(T - T_{VF})} \tag{3}$$

where U is activation energy, k_B is Boltzmann constant, and T_{VF} is an arbitrary reference temperature. For the thermally annealed terpolymer, the parameters by curve fitting are $U =$

15 meV (0.4 kcal/mol), $T_{VF} = 282$ K, and $f_0 = 4.1 \times 10^7$ Hz. The thermal activation energy is too small to be expected for a relaxation associated with the glass transition and would have contributions from short-range molecular motions in the crystalline phase. Since the relaxor has short all-trans ($T_{m>4}$) conformations interrupted by the TG/TG′ conformations, its response to external field is assumed to occur by the propagation of structure defects (TG) along the skeletal chain in a mechanism similar to that of poling PVDF.[40] The crystal cohesive energies of $T_{m>4}$ and T_3GT_3G' crystalline phases of P(VDF−TrFE) are −0.86 and −1.23 kcal/mol per carbon atom,[31] which suggests that motion of structure defects in the terpolymer is low-energy consumption.

On the basis of these analyses, it is reasonable to rule out the contribution of micro-Brownian motion of chains in amorphous phase to the relaxor behavior in the terpolymers. For the frequency-dependent structure transition peak around 10 °C in the relaxor terpolymer (thermally annealed sample) observed in DMTA, there are several features: (1) The structural phase transition temperature is well below Curie temperature, indicating that the polar crystalline domains are less stable and include more structure defects (gauche conformation) than the well-ordered or less-ordered ferroelectrics. The polar regions disappear and transform into a nonpolar paraelectric phase at a certain temperature. (2) The relaxor state may be the consequence of the nanosize effect. The ferroelectric phases are substituted by relaxor states whenever they reduce to a critical size. It is quantified by coherence length of less than 4.7 nm, roughly estimated by eq 2 with $T_c < 10$ °C. The effect is contributed to increased volume fraction of surface layer on ferroelectric nanodomains. The surface energy increment cannot be readily covered by the reduction of bulk free energy interrelated with polar nanodomains formation. One also expects that the dimension of the polar domain will be the key to the overall performance of the terpolymers varying from normal ferroelectrics to relaxor ferroelectrics. This kind of nanosize effect has been demonstrated earlier in typical relaxor ferroelectrics. In PMN, it has been shown that the critical correlation length is of the order of 20 nm.[41,42] If the correlation length becomes higher than this value, below the freezing temperature, the polydispersive dynamics disappear (nonergodic behavior) and the system behaves like a normal ferroelectric. On the other hand, on heating the sample the correlation length decreases continuously down to 5 nm, leading to the relaxor (ergodic) behavior. (3) For the thermally annealed terpolymer, the paraelectric phase is predominant in crystalline regions. Therefore, the polar clusters of nanometer scale disperse within the paraelectric matrix, where each of them behaves as a dipolar entity with a single relaxation time. However, polar nanodomains are randomly orientated, have a wide distribution in the size, and can interact with each other. Relaxation processes are associated with the domain reorientation or domain wall motion. Therefore, a broad distribution of relaxation times is expected and responsible for frequency dependence of the dielectric and mechanical behaviors in these materials.

Conclusions

High termonomer content in fluorinated terpolymer is usually considered to be adverse to the formation ferroelectric phases. However, by lowering the crystallization temperature, the ferroelectric-like phase in P(VDF−TrFE−CFE) with 8.2 mol % CFE can be induced and even overwhelm the paraelectric one. Besides crystal melting, there are at least three transitions taking place in terpolymers SG30 and SG60. The phase transitions from less-ordered or well-ordered ferroelectrics to paraelectrics in crystalline region give one or two endothermal peaks between 30 and 90 °C and cause significant changes in XRD and FTIR spectra. The glass transition originating from micro-Brownian motion in amorphous region is identified to happen at temperature below −20 °C. The most attractive structure transition occurs near 10 °C and root from crystals with all-trans sequence randomly disrupted by gauche conformation. These polar domains are intermediate state between ferroelectrics and paraelectrics with coherence length of less than 4.7 nm. Both ferroelectric phase and polar nanodomain contribute to the extremely large dielectric response of the terpolymers with respect to other polymer including P(VDF−TrFE) copolymers. The former is in charge of the nearly frequency-independent dielectric maxima (sharp phase transition), and the latter leads to strongly frequency dependence of dielectric spectra (diffuse phase transition). This strongly suggests the characteristic of ferroelectric relaxor comes from the short-range molecular motion in the polar nanodomain.

Acknowledgment. This work is supported by the National Natural Science Foundation of China under Contracts 20574035 and 50228304.

References and Notes

(1) Uchino, K. *Ferroelectric Devices*; Marcel Dekker: New York, 2000.
(2) Damjanovic, D. *Rep. Prog. Phys.* **1998**, *61*, 1267−1324.
(3) Park, B. H.; Kang, B. S.; Bu, S. D.; Noh, T. W.; Lee, J.; Jo, W. *Nature (London)* **1999**, *401*, 682−684.
(4) Ahn, C. H.; Rabe, K. M.; Triscone, J.-M. *Science* **2004**, *303*, 488−491.
(5) Tsymbal, E. Y.; Kohlstedt, H. *Science* **2006**, *313*, 181−183.
(6) Nalwa, H. S. *Ferroelectric Polymers: Chemistry, Physics, and Applications*; Marcel Dekker: New York, 1995.
(7) Lovinger, A. J. *Science* **1983**, *220*, 1115−1121.
(8) Kawai, H. *Jpn. J. Appl. Phys.* **1969**, *8*, 975−976.
(9) Bergman, J. G.; McFee, J. H.; Crane, G. R. *Appl. Phys. Lett.* **1971**, *18*, 203−205.
(10) Tamura, M.; Ogasawara, K.; Ono, N.; Hagiwara, S. *J. Appl. Phys.* **1974**, *45*, 3768−3771.
(11) Yagi, T.; Tatemoto, M.; Sako, J. *Polym. J.* **1980**, *12*, 209−223.
(12) Bune, A. V.; Fridkin, V. M.; Ducharme, S.; Blinov, L. M.; Palto, S. P.; Sorokin, A. V.; Yudin, S. G.; Zlatkin, A. *Nature (London)* **1998**, *391*, 874−877.
(13) Zhang, Q. M.; Bharti, V.; Zhao, X. *Science* **1998**, *280*, 2101−2104.
(14) Chu, B.; Zhou, X.; Ren, K.; Neese, B.; Lin, M.; Wang, Q.; Bauer, F.; Zhang, Q. M. *Science* **2006**, *313*, 334−336.
(15) Lovinger, A. J.; Davis, G. T.; Furukawa, T.; Broadhurst, M. G. *Macromolecules* **1982**, *15*, 323−328.
(16) Chung, T. C.; Petchsuk, A. *Mater. Res. Soc. Symp. Proc.* **2000**, *600*, 53−60.
(17) Chung, T. C.; Petchsuk, A. U.S. Patent 6,355,749, 2002.
(18) Xu, H.; Cheng, Z. Y.; Olson, D.; Mai, T.; Zhang, Q. M.; Kavarnos, G. *Appl. Phys. Lett.* **2001**, *78*, 2360−2362.
(19) Xia, F.; Cheng, Z.-Y.; Xu, H.; Li, H.; Zhang, Q. M.; Kavarnos, G. J.; Ting, R. Y.; Abdel-Sadek, G.; Belfield, K. D. *Adv. Mater.* **2002**, *14*, 1574−1577.
(20) Chung, T. C.; Petchsuk, A. *Macromolecules* **2002**, *35*, 7678−7684.
(21) Cross, L. E. *Ferroelectrics* **1994**, *151*, 305−320.
(22) Blinc, R.; Dolinsek, J.; Gregorovic, A.; Zalar, B.; Filipic, C.; Kutnjak, Z.; Levstik, A.; Pirc, R. *Phys. Rev. Lett.* **1999**, *83*, 424−427.
(23) Samara, G. A. *J. Phys.: Condens. Matter* **2003**, *15*, R367−411.
(24) Bokov, A. A.; Ye, Z. G. *J. Mater. Sci.* **2006**, *41*, 31−52.
(25) Viehland, D.; Jang, S. J.; Cross, L. E.; Wuttig, M. *Phys. Rev. B* **1992**, *46*, 8003−8006.
(26) Klein, R. J.; Runt, J.; Zhang, Q. M. *Macromolecules* **2003**, *36*, 7220−7226.
(27) Zhang, S.; Chu, B.; Neese, B.; Ren, K.; Zhou, X.; Zhang, Q. M. *J. Appl. Phys.* **2006**, *99*, 044107.
(28) Ang, C.; Yu, Z. *Appl. Phys. Lett.* **2005**, *86*, 262903.
(29) Klein, R. J.; Xia, F.; Zhang, Q. M.; Bauer, F. *J. Appl. Phys.* **2005**, *97*, 094105.
(30) Bauer, F.; Fousson, E.; Zhang, Q. M.; Lee, L. M. *IEEE Trans. Dielectr. Electr. Insul.* **2004**, *11*, 293−298.

(31) Su, H.; Strachan, A.; Goddard, III, W. A. *Phys. Rev. B* **2004**, *70*, 064101.
(32) Tashiro, K.; Takano, K.; Kobayashi, M.; Chatani, Y.; Tadokoro, H. *Polymer* **1984**, *25*, 195−208.
(33) Benz, M.; Euler, W. B.; Gregory, O. J. *Macromolecules* **2002**, *35*, 2682−2688.
(34) Salimi, A.; Yousefi, A. A. *J. Polym. Sci., Part B: Polym. Phys.* **2004**, *42*, 3487−3495.
(35) Kobayashi, M.; Tashiro, K.; Tadokoro, H. *Macromolecules* **1975**, *8*, 158−171.
(36) Tashiro, K.; Kobayashi, M.; Tadokoro, H. *Macromolecules* **1981**, *14*, 1757−1764.
(37) Tashiro, K.; Itoh, Y.; Kobayashi, M.; Tadokoro, H. *Macromolecules* **1985**, *18*, 2600−2606.
(38) Zhong, W. L.; Wang, Y. G.; Zhang, P. L.; Qu, B. D. *Phys. Rev. B* **1994**, *50*, 698−703.
(39) Li, G. R.; Kagami, N.; Ohigashi, H. *J. Appl. Phys.* **1992**, *72*, 1056−1061.
(40) Dvey-Aharon, H.; Sluckin, T. J.; Taylor, P. L.; Hopfinger, A. J. *Phys. Rev. B* **1980**, *21*, 3700−3707.
(41) Welter, C.; Faria, L. O.; Moreira, R. L. *Phys. Rev. B* **2003**, *67*, 144103.
(42) Viehland, D.; Wuttig, M.; Cross, L. E. *Ferroelectrics* **1991**, *120*, 71−77.

MA062800L